The Many Phases of Strongly Interacting Matter

Alejandro Ayala
Instituto de Ciencias Nucleares,
Universidad Nacional Autónoma de México

XVIII Mexican Workshop on Particles and Fields
November 2022

Phase transitions

What is a phase transition?

- Transformation of a given substance from one state of matter to another.
- During the phase transition some quantities change, often in a discontinuous manner.
- Changes result in variations of external conditions such as pressure, temperature, etc.

Phase transitions

When does a phase transition happen?

- In technical terms, they occur when the **free energy is non-analytic (one of its derivatives diverges)** for some values of the thermodynamical variables.
- They result from the interaction of a **large number of particles** and in general it does not occur when the system is very small or has a small number of particles.
- On the phase transition lines **the free energies in both phases coincide.**
- Some times it is possible to change the state of a substance without crossing a phase transition line. Under these conditions one talks about a **crossover transition.**

QCD: The theory of strong interactions

- Gauge theory with the **local** symmetry group $SU(N_c)$. (In the real world $N_c = 3$).
- The fundamental fields are the **quarks** (matter fields) and **gluons** gauge fields.
- Each one of the N_f **quark fields** belong to the **fundamental representation** of the color group which is (N_c)–dimensional, **antiquark fields** to the **complex conjugate of the fundamental representation**, also (N_c)–dimensional and **gluon fields** to the adjoint representation which is $(N_c^2 - 1)$–dimensional.

$$\mathcal{L}_{QCD} = \sum_{i=1}^{N_f} \overline{\psi}_i^a \left(i\gamma^\mu (\partial_\mu \delta^{ab} + i g_s A_\mu^{ab}) - m_i \delta^{ab} \right) \psi_i^b - \frac{1}{4} G_{\mu\nu}^\alpha G_\alpha^{\mu\nu};$$

$$G_{\mu\nu}^\alpha = \partial_\mu A_\nu^\alpha - \partial_\nu A_\mu^\alpha + g_s f^{\alpha\beta\sigma} A_\mu^\beta A_\nu^\sigma; \qquad A_\mu^{ab} = A_\mu^\sigma (\tau_\sigma)^{ab}$$

a, b run from 1 to N_c, $\alpha,\ \beta,\ \sigma$ run from 1 to $N_c^2 - 1$.

The QCD phase diagram

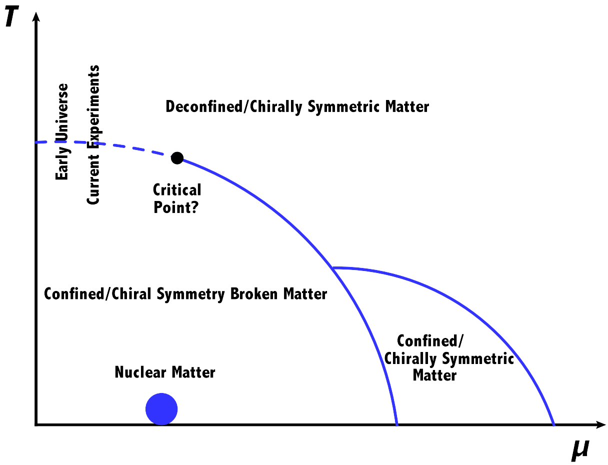

The QCD phase diagram

- Since the coupling constant runs towards smaller values with increasing energy scale **it is natural to anticipate that confined and chiral symmetry broken QCD matter undergoes a phase transition at high energy densities,** $T \simeq \Lambda_{QCD} \sim 200$ MeV, $n_B \simeq \Lambda_{QCD}^3 \sim 1\ \mathrm{fm}^{-3}$.

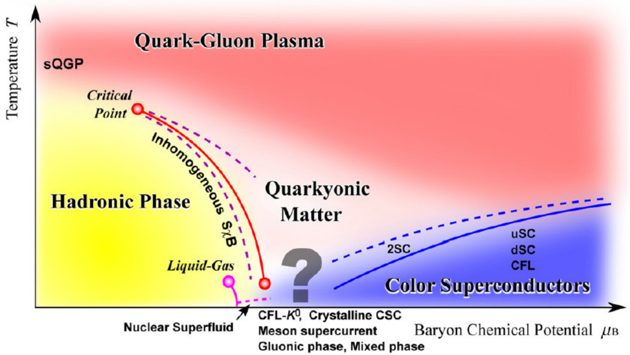

New multimessenger era

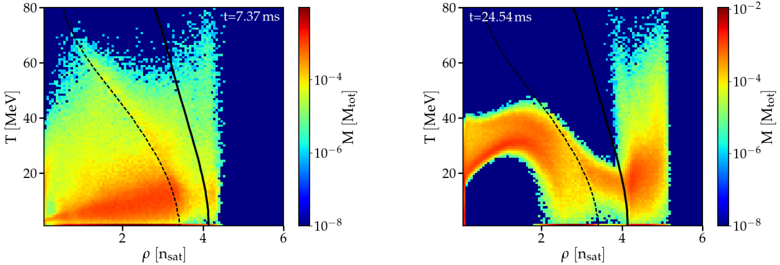

Population of the QCD phase diagram by a typical merger event of two neutron stars with 1.35 $M_\odot$ each, for $t = 7.37$ ms (left panel) and $t = 24.54$ ms (right panel) after the merging.

The extended QCD phase diagram

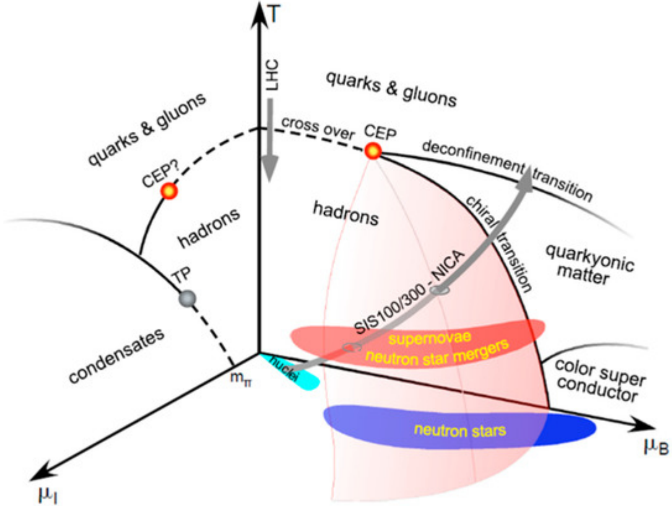

Heavy-Ion Physics

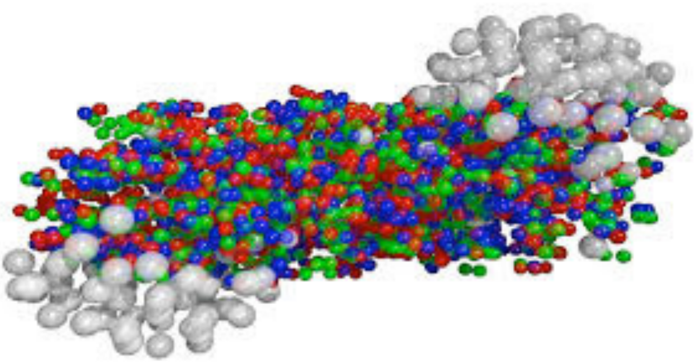

Phase diagram explored with Heavy-Ion collisions

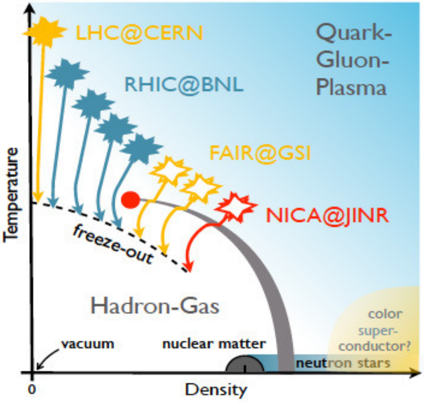

Phase diagram explored with Heavy-Ion collisions

Our current knowledge of the phase diagram is restricted to near the Temperature-axis.

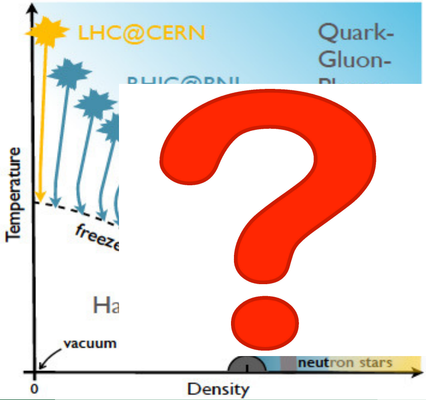

Chiral symmetry restoration

- The QCD vacuum within hadrons should be regarded as a medium responsible for the non-perturbative quark mass.
- In hot and/or dense energetic matter quarks turn bare due to asymptotic freedom.
- **We expect a phase transition from a state with heavy constituent quarks to another with light current quarks.**
- The transition is called **chiral phase transition.**

Is there a Critical End Point?

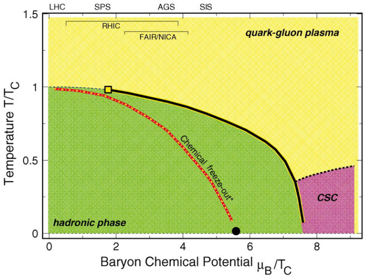

- Most of the **effective models** suggest the existence of a QCD critical point $(\mu_{\mathrm{CEP}}, T_{\mathrm{CEP}})$ somewhere in the middle of the phase diagram **where the crossover line becomes a first order transition line.**
- Signals are and will be looked for in current and future facilities.

Lattice QCD pseudo-critical transition

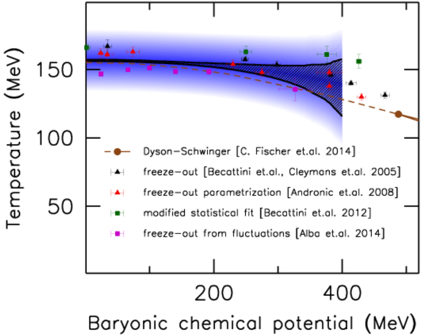

R. Bellwiede, *et al.*, Phys. Lett. B **751**, 559-564 (2015).

Lattice QCD Critical End Point

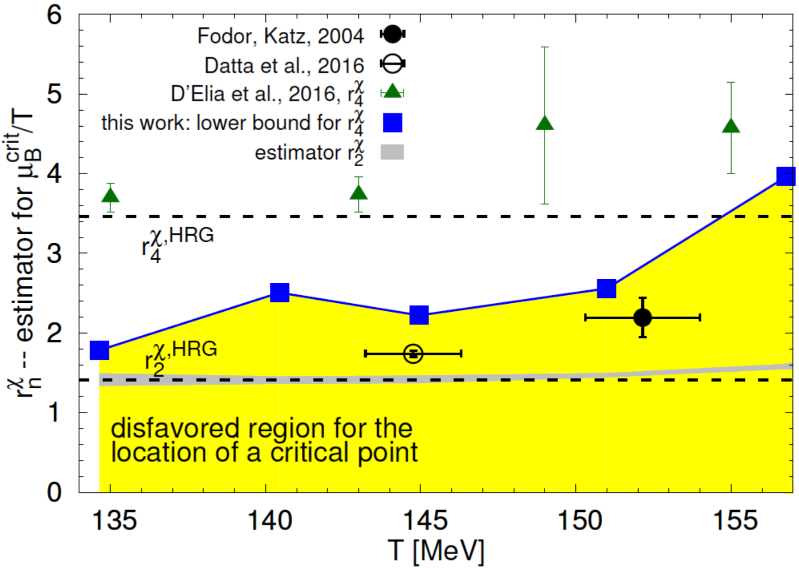

Analysis tools: Fluctuations of conserved quantities

- A powerful tool to experimentally locate the CEP is the study of **event-by-event fluctuations** in relativistic heavy-ion collisions

Fluctuations are sensitive to the early thermal properties of the created medium. In particular, the possibility to detect **non Gaussian fluctuations** in conserved charges is one of the central topics in this field

Analysis tools: Cumulant generating function

- The relation with thermodynamics comes through the partition function $\mathcal{Z}$, which is the fundamental object

The partition function is also the moment generating function and therefore **the cumulant generating function is given by** $\ln \mathcal{Z}$

- Cumulants are extensive quantities. Consider the number N of a conserved quantity in a volume V in a grand canonical ensemble. It can be shown that its cumulant of order n can be written as

$$\langle N^n \rangle_{c,V} = \chi_n V$$

χ_n are called the **generalized susceptibilities**

Analysis tools: Cumulant generating function

Cumulants higher than second order vanish for a Gaussian probability distribution, non-Gaussian fluctuations are signaled by non-vanishing higher order cumulants

Two important higher order moments are the **skewness** S and the **curtosis** κ. The former measures the asymmetry of the distribution function whereas the latter measures its sharpness

Fluctuations of conserved quantities

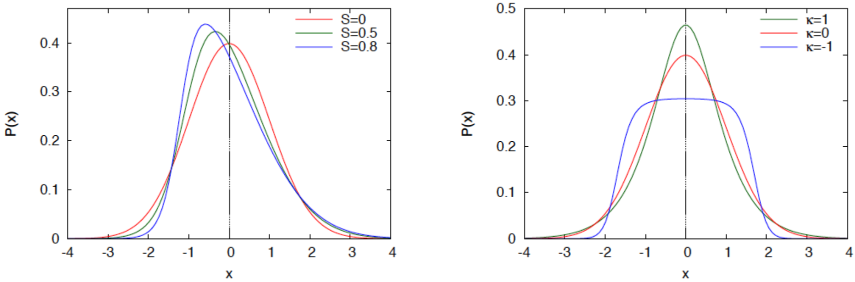

Analysis tools: Cumulant generating function

When the stochastic variable x is normalized to the square root of the variance, σ, such that $x \to \tilde{x} = x/\sigma$, the skewness and the kurtosis are given as the third and fourth-order cumulants

$$S = \langle \tilde{x}^3 \rangle_c, \qquad \kappa = \langle \tilde{x}^4 \rangle_c$$

Cumulants

For the HRGM,
ratios of cumulatns of even order are equal to 1

In particular, for the square of the variance σ^2 and the kurtosis κ

$$\langle N^4 \rangle_c / \langle N^2 \rangle_c = \kappa\sigma^2$$

Look for deviations from 1 in $\kappa\sigma^2$ as a function of collision energy as a signal of the CEP.

Linear sigma model with quarks

$$
\begin{aligned}
\mathcal{L} &= \frac{1}{2}(\partial_\mu \sigma)^2 + \frac{1}{2}(\partial_\mu \vec{\pi})^2 + \frac{a^2}{2}(\sigma^2 + \vec{\pi}^2) \\
&- \frac{\lambda}{4}(\sigma^2 + \vec{\pi}^2)^2 + i\bar{\psi}\gamma^\mu \partial_\mu \psi - g\bar{\psi}(\sigma + i\gamma_5 \vec{\tau}\cdot\vec{\pi})\psi, \\
\sigma &\to \sigma + v \\
\mathcal{L} &= \frac{1}{2}(\partial_\mu \sigma)^2 + \frac{1}{2}(\partial_\mu \vec{\pi})^2 - \frac{1}{2}\left(3\lambda v^2 - a^2\right)\sigma^2 \\
&- \frac{1}{2}\left(\lambda v^2 - a^2\right)\vec{\pi}^2 \\
&+ \frac{a^2}{2}v^2 - \frac{\lambda}{4}v^4 + i\bar{\psi}\gamma^\mu \partial_\mu \psi - gv\bar{\psi}\psi + \mathcal{L}_I^b + \mathcal{L}_I^f \\
\mathcal{L}_I^b &= -\frac{\lambda}{4}\Big[(\sigma^2 + (\pi^0)^2)^2 + 4\pi^+\pi^-(\sigma^2 + (\pi^0)^2 + \pi^+\pi^-)\Big], \\
\mathcal{L}_I^f &= -g\bar{\psi}(\sigma + i\gamma_5 \vec{\tau}\cdot\vec{\pi})\psi
\end{aligned}
$$

Thermodynamics from the effective potential

$$\mathcal{Z}(T, v) = \exp\left\{-\Omega V^{\text{eff}}(v)/T\right\}$$

Effective potential

$$
\begin{aligned}
V^{\rm eff} &= V^{\rm tree} + V^{\rm b} + V^{\rm f} + V^{\rm Ring} \\
V^{\rm tree}(v) &= -\frac{a^2}{2}v^2 + \frac{\lambda}{4}v^4 \\
V^{\rm b}(v,T) &= T\sum_n \int \frac{d^3k}{(2\pi)^3} \ln D_{\rm b}(\omega_n,\vec{k})^{1/2} \\
V^{\rm f}(v,T,\mu) &= -T\sum_n \int \frac{d^3k}{(2\pi)^3} {\rm Tr}[\ln S_{\rm f}(\tilde{\omega}_n,\vec{k})^{-1}] \\
V^{\rm Ring}(v,T,\mu) &= \frac{T}{2}\sum_n \int \frac{d^3k}{(2\pi)^3} \ln[1+\Pi_{\rm b} D(\omega_n,\vec{k})] \\
\Pi_{\rm b} &\equiv \Pi_\sigma = \Pi_{\pi^\pm} = \Pi_{\pi^0} \\
&= \lambda\frac{T^2}{2} - N_{\rm f}N_{\rm c}g^2\frac{T^2}{\pi^2}\left[{\rm Li}_2\left(-e^{-\frac{\mu}{T}}\right) + {\rm Li}_2\left(-e^{\frac{\mu}{T}}\right)\right]
\end{aligned}
$$

Plasma screening in TFT: Ring diagrams

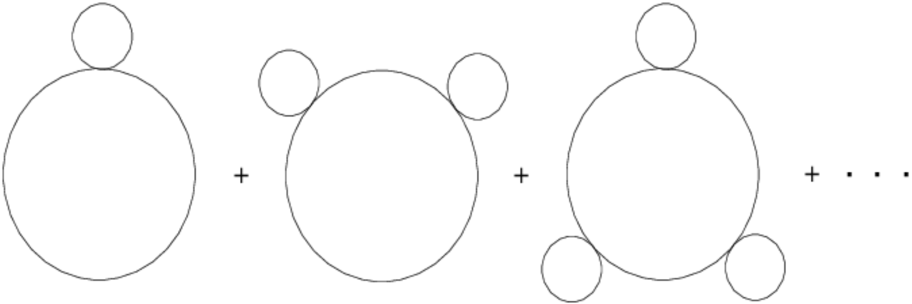

Effective potential

$$
\begin{aligned}
V^{\text{eff}}(v) &= -\frac{a^2}{2}v^2 + \frac{\lambda}{4}v^4 \\
&+ \sum_{\text{b}=\pi^\pm,\pi^0,\sigma} \left\{ -\frac{T^4\pi^2}{90} + \frac{T^2 m_{\text{b}}^2}{24} - \frac{T(m_{\text{b}}^2+\Pi_{\text{b}})^{3/2}}{12\pi} \right. \\
&- \left. \frac{m_{\text{b}}^4}{64\pi^2}\ln\left(\frac{\tilde{\mu}^2}{T^2}\right) \right\} \\
&+ N_{\text{c}}N_{\text{f}} \left\{ \frac{m_f^4}{16\pi^2}\left[\ln\left(\frac{\tilde{\mu}^2}{T^2}\right) - \psi^0\left(\frac{1}{2}+\frac{i\mu}{2\pi T}\right) - \psi^0\left(\frac{1}{2}-\frac{i\mu}{2\pi T}\right) \right.\right. \\
&+ \left. \psi^0\left(\frac{3}{2}\right) - 2\left(1+\ln(2\pi)\right) + \gamma_E \right] \\
&- \frac{m_{\text{f}}^2 T^2}{2\pi^2}\left[\text{Li}_2\left(-e^{-\frac{\mu}{T}}\right) + \text{Li}_2\left(-e^{\frac{\mu}{T}}\right) \right] \\
&+ \left. \frac{T^4}{\pi^2}\left[\text{Li}_4\left(-e^{-\frac{\mu}{T}}\right) + \text{Li}_4\left(-e^{\frac{\mu}{T}}\right) \right] \right\}
\end{aligned}
$$

Effective potential

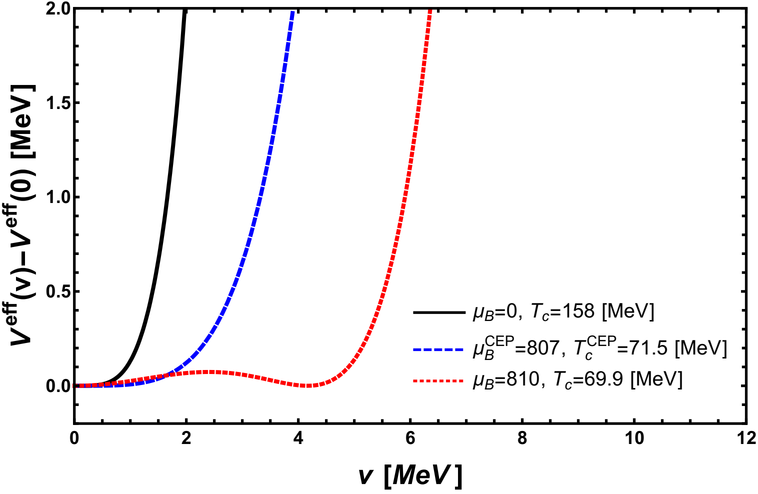

Partition function in the LSMq up to ring diagram order

$$\mathcal{Z}(v) = \exp\left\{-\Omega V^{\text{eff}}(v)/T\right\}$$

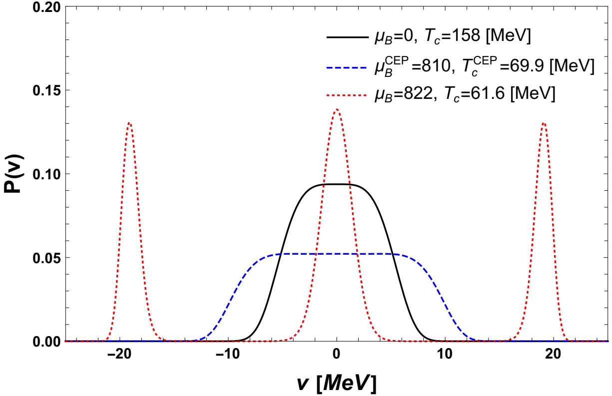

Baryon number fluctuations in the LSMq up to ring diagram order; curtosis

$$\mathcal{Z}(v) = \exp\left\{-\Omega V^{\text{eff}}(v)/T\right\}$$

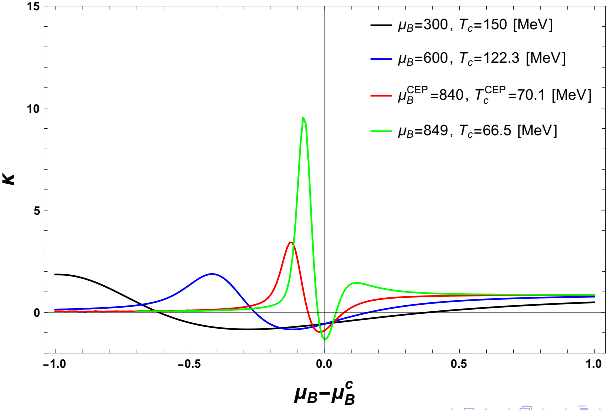

Effective phase diagram

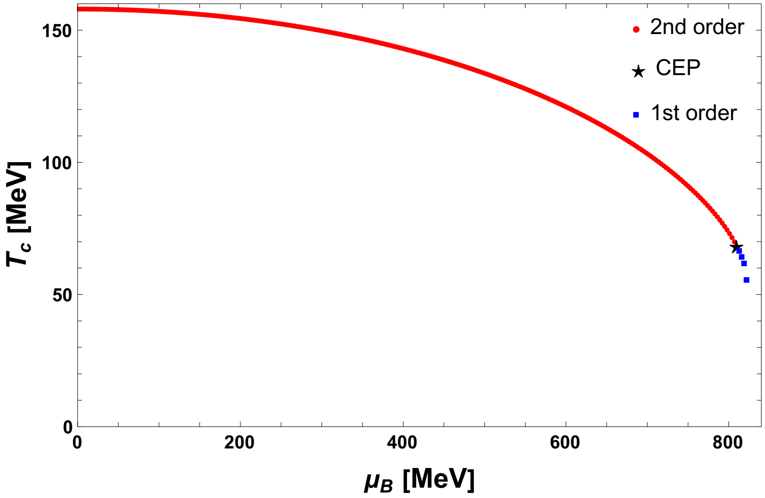

Freeze-out line Randrup & Cleymans, PRC **74**, 047901 (2006)

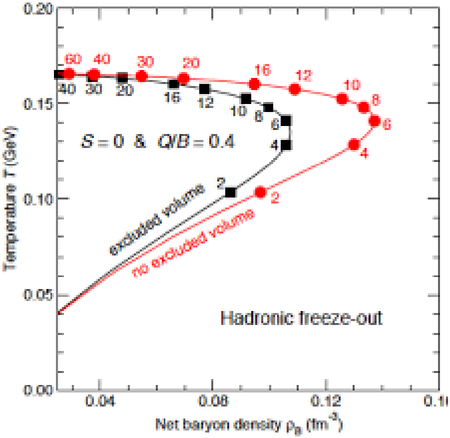

$$\mu_B(\sqrt{s_{NN}}) = \frac{d}{1 + e\sqrt{s_{NN}}} \quad d = 1.308\text{GeV}, \; e = 0.273\text{GeV}^{-1}$$

Baryon number fluctuations in the LSMq

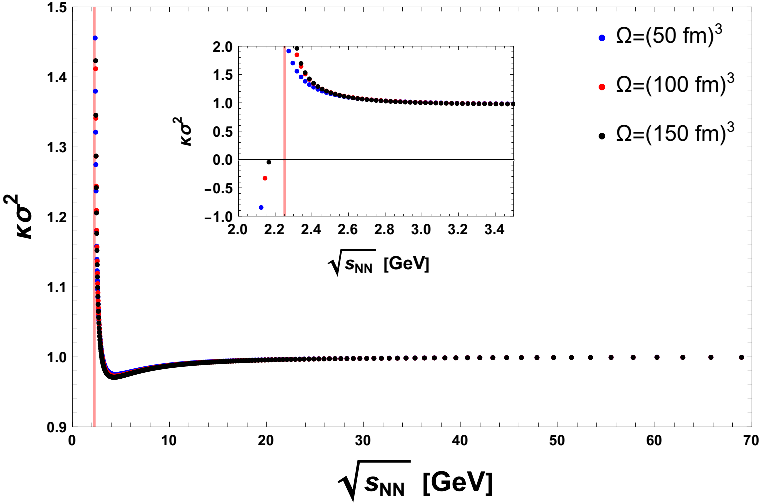

STAR and HADES recent results

Result 1: Net-proton C_4/C_2 from BES-I

J. Adam *et al.* (STAR Collaboration) Phys. Rev. Lett. **126**, 092301; long version paper: arXiv:2101.12413

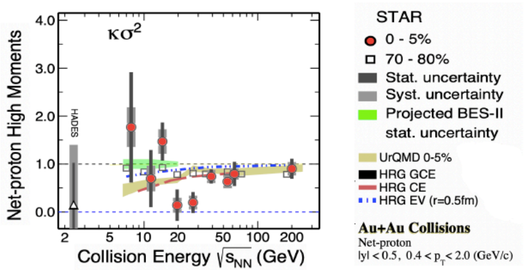

- Non-monotonic energy dependence of net-proton $\kappa\sigma^2$ is shown in top 5% from BES-I data which is not reproduced by various models.
- More statistics below 20 GeV are needed to confirm the non-monotonic trend.
- Measurement from new dataset in fixed target experiment at $\sqrt{s_{NN}} = 3$ GeV is on the way!

2021/4/2 55th Rencontres de Moriond 2021 10

Dedicated experiments to explore QCD phase diagram

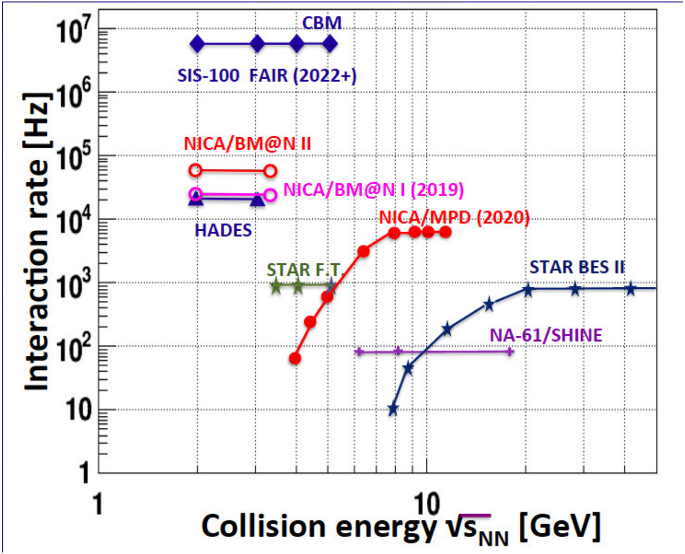

Multi-Purpose Detector (MPD) Collaboration

MPD** International Collaboration was established in **2018
to construct, commission and operate the detector

10** Countries, **>450** participants, **31** Institutes and **JINR

Organization

Acting Spokesperson:	***Victor Riabov***
Deputy Spokesperson:	***Zebo Tang***
Institutional Board Chair:	***Alejandro Ayala***
Project Manager:	***Slava Golovatyuk***

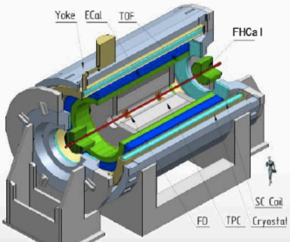

Joint Institute for Nuclear Research;
*AANL, Yerevan, **Armenia;***
*University of Plovdiv, **Bulgaria;***
*Tsinghua University, Beijing, **China**;*
*USTC, Hefei, **China**;*
*Huzhou University, Huizhou, **China**;*
*Institute of Nuclear and Applied Physics, CAS, Shanghai, **China**;*
*Central China Normal University, **China**;*
*Shandong University, Shandong, **China**;*
*IHEP, Beijing, **China**;*
*University of South China, **China**;*
*Three Gorges University, **China**;*
*Institute of Modern Physics of CAS, Lanzhou, **China**;*
*Tbilisi State University, Tbilisi, **Georgia**;*
*FCFM-BUAP (Heber Zepeda) Puebla, **Mexico**;*
*FC-UCOL (Maria Elena Tejeda), Colima, **Mexico**;*
*FCFM-UAS (Isabel Dominguez), Culiacán, **Mexico**;*
*ICN-UNAM (Alejandro Ayala), Mexico City, **Mexico**;*
*Institute of Applied Physics, Chisinev, **Moldova**;*
*Institute of Physics and Technology, **Mongolia**;*

*Belgorod National Research University, **Russia**;*
*INR RAS, Moscow, **Russia**;*
*MEPhI, Moscow, **Russia**;*
*Moscow Institute of Science and Technology, **Russia**;*
*North Osetian State University, **Russia**;*
*NRC Kurchatov Institute, ITEP, **Russia**;*
*Kurchatov Institute, Moscow, **Russia**;*
*St. Petersburg State University, **Russia**;*
*SINP, Moscow, **Russia**;*
*PNPI, Gatchina, **Russia**;*
*Vinča Institute of Nuclear Sciences, **Serbia**;*
*Pavol Jozef Šafárik University, Košice, **Slovakia***

NICA Complex JINR

NICA Accelerator Complex in Dubna

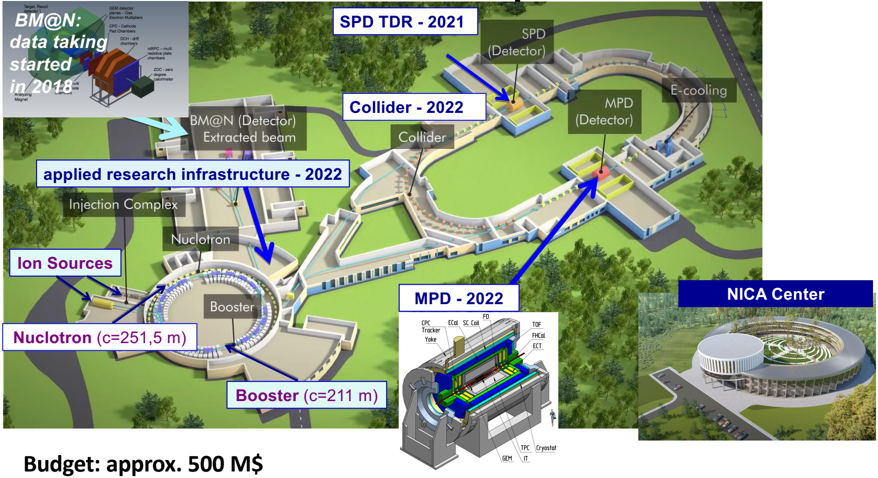

Budget: approx. 500 M$

MPD Schedule (see V. Riabov's talk)

NICA

MPD schedule

- Latest estimates provided by V. Golovatyuk (subject to change)

	Year 2022	
8	Jan 20 - April 30	Cables for Solenoid probes signals installation
9	May 16 - Dec 25th	Assembling Iron yoke, Cryogenic platform and Cryostat. New LHe and LN pipes ordering
10	Sept - Dec 30	Cryogenic infrastructure for cooling down by temporary scheme, power Supply and Control system preparation
	Year 2023	
11	Jan 15 - February 15th	Vacuum test of Solenoid with Cryostat
12	Feb 15 - April 20	Solenoid cooling down to Liquid Helium temperature
13	May 10 - July 20	Magnetic Field measurements
14	July 25 - August 10	Support Frame installation
15	August 20 – Sept 30th	Installation ECal sectors, Moving Platforms mounting
16	Sept 17 – Oct 10th	Installation TOF modules, FHCal into poles
17	Oct 11 - Nov 30	TPC installation
18	Sept 18 - Nov 30	Cabling
19	Dec 4 - Dec 25	Installation of beam pipe
	Year 2024	
20	Jan 10 - Feb	Switching on the MPD, Commissioning

- Preparation of the MPD detector and experimental program is ongoing, all activities are continued
- All components of the MPD 1-st stage detector are in advanced state of production (subsystems, support frame, electronics platforms, LV/HV, control systems, cryogenics, cabling, etc.)

MPD Collaboration

Summary

- Rich structure of the QCD phase diagram
- International interest in the field shows up in the several present and future experiments designed to explore the properties of strongly interacting matter subject to extreme conditions
- Deviations from HRG behavior when using LSMq as an effective QCD model up to **ring diagrams contribution.**
- Ring diagrams inclusion is equivalent to introducing screening effects at finite T and μ_B.
- CEP signaled by divergence of $\kappa\sigma^2$
- 786 MeV $< \mu_B^{\text{CEP}} <$ 849 MeV and $T^{\text{CEP}} \sim$ 70.3 MeV
- CEP found at low T and high μ_B (NICA, HADES?)

¡Muchas Gracias!

BACKUP

Analysis tools: Fluctuations of conserved quantities

- For a probability distribution function $\mathcal{P}(x)$ of an stochastic variable x, the moments are defined as

$$\langle x^n \rangle = \int dx \, x^n \mathcal{P}(x)$$

- We can define the **moment generating function** $G(\theta)$ as

$$G(\theta) = \int dx \, e^{x\theta} \mathcal{P}(x)$$

- from where

$$\langle x^n \rangle = \frac{d^n}{d\theta^n} G(\theta) \Big|_{\theta=0}$$

Analysis tools: Cumulant generating function

$$K(\theta) = \ln G(\theta)$$

- The cumulants of $\mathcal{P}(x)$ are defined by

$$\begin{aligned}
\langle x^n \rangle_c &= \left. \frac{d^n}{d\theta^n} K(\theta) \right|_{\theta=0}, \\
\langle x \rangle_c &= \langle x \rangle, \\
\langle x^2 \rangle_c &= \langle x^2 \rangle - \langle x \rangle^2 = \langle \delta x^2 \rangle, \\
\langle x^3 \rangle_c &= \langle \delta x^3 \rangle, \\
\langle x^4 \rangle_c &= \langle \delta x^4 \rangle - 3\langle \delta x^2 \rangle^2.
\end{aligned}$$

Analysis tools: Fluctuations of conserved quantities

- For example, the variance of Q is given

$$\langle \delta Q^2 \rangle_\Omega = \langle (Q - \langle Q \rangle_V)^2 \rangle_\Omega = \int_V dx_1 dx_2 \langle \delta n(x_1) \delta n(x_2) \rangle$$

- The integrand on the right-hand side is called a **correlation function**, whereas the left-hand side is called a (second order) **fluctuation**

We see that fluctuations are closely related to correlation functions

In relativistic heavy-ion collisions, fluctuations are measured on an event-by-event basis in which the number of some charge or particle species is counted in each event

Higher moments, larger sensitivity to correlation length ξ

- In HIC's, the simplest measurements of fluctuations are event-by-event variances in observables such as multiplicities or mean transverse momenta of particles.
- At the CEP, these variances diverge approximately as ξ^2. **They manifest as a non-monotonic behavior as the CEP is passed by during a beam energy scan.**
- In a realistic HIC, the divergence of ξ is tamed by the effects of *critical slow down* (the phenomenon describing a finite and possibly large relaxation time near criticality).
- However, higher, non-Gaussian moments of the fluctuations depend much more sensitively on ξ.
- **Important to look at the Kurtosis κ (proportional to the fourth-order cumulant C_4), which grows as ξ^7.**

Analysis tools: Cumulant generating function

- The relation with thermodynamics comes through the partition function $\mathcal{Z}$, which is the fundamental object

The partition function is also the moment generating function and therefore **the cumulant generating function is given by** $\ln \mathcal{Z}$

- Cumulants are extensive quantities. Consider the number N of a conserved quantity in a volume Ω in a grand canonical ensemble. It can be shown that its cumulant of order n can be written as

$$\langle N^n \rangle_{c,\Omega} = \chi_n \Omega$$

χ_n are called the **generalized susceptibilities**

Susceptibilities

- Experimentally it is easier to measure the **central moments** M: $M_{BQS}^{ijk} = \langle (B - \langle B \rangle)^i (Q - \langle Q \rangle)^j (S - \langle S \rangle)^k \rangle$.
- On the other hand, derivatives of $\ln \mathcal{Z}$ with respect to the chemical potentials give the susceptibilities χ:

$$\chi_{BQS}^{ijk} = \frac{\partial^{i+k+j}(P/T^4)}{\partial^i(\mu_B/T)\partial^j(\mu_Q/T)\partial^k(\mu_S/T)}; \quad P = \frac{T}{\Omega} \ln \mathcal{Z}.$$

$$\Longrightarrow \chi_{XY} = \frac{1}{\Omega} T^3 M_{XY}^{11}$$

Fixing the parameters a^2, λ and g from LQCD Phys. Rev. Lett. **125**, 052001 (2020)

At the phase transition, the effective potential is flat at $v = 0$. This property can be exploited to find the suitable values of the model parameters a, λ and g at the critical temperature T_c for $\mu_B = 0$

$$6\lambda \left(\frac{T_c^2}{12} - \frac{T_c}{4\pi} \left(\Pi_{\mathrm{b}}(T_c, \mu_B = 0) - a^2 \right)^{1/2} + \frac{a^2}{16\pi^2} \left[\ln \left(\frac{\tilde{\mu}^2}{T_c^2} \right) \right] \right) + g^2 T_c^2 - a^2 = 0.$$

$$\frac{T_c(\mu_B)}{T_c} = 1 - \kappa_2 \left(\frac{\mu_B}{T_c} \right)^2 + \kappa_4 \left(\frac{\mu_B}{T_c} \right)^4 ,$$